All-printed Paper Based Supercapacitors

Lu Shi, Yang Wang, Wenhui Lai, Zhi Jiang, Ronghe Wang, Cheng Yang*
Division of Energy and Environment, Graduate School at Shenzhen, Tsinghua University
Xili University Town, Shenzhen, China
yang.cheng@sz.tsinghua.edu.cn

***Abstract*—With the rapid development of portable electronics, such as e-paper and other flexible devices, power sources with a high flexibility become an important prerequisite. In this run, supercapacitors with a small form factor are recently emerging as a competitive candidate. Here, we introduce an all-printed paper based supercapacitor (PPS) assembled by screen printing and stencil printing technology, which shows superior electrochemical performance; moreover, it is compatible with mass production processes. The key electrode material, δ-MnO_2 nanosheets, synthesized by one-step synthetic process exhibit a high specific capacitance of 120 F g^{-1}. Using this δ-MnO_2 nanosheets electrode material and aqueous electrolyte, the capacity of the device could reach 4.7 mF g^{-1} with the volume of 2.0*1.7*0.2mm^3. More important, the supercapacitor is lightweight and miniaturized, which can well cater to the development of future wearable electronics.**

Keywords—supercapacitors, all-printed, paper based, miniaturized

I. INTRODUCTION

Ever increasing energy demand worldwide on limited fossil fuel resources has accelerated the pursuit of alternative energy conversion/storage systems such as solar cells, secondary lithium-ion batteries[1] and supercapacitors.[2-5] Supercapacitors as a new type of energy storage device gradually play an indispensable role in industry owing to many intriguing characteristics, such as high power density, fast charge and discharge rate and long cycle life. However, devices are often fabricated by spray-coating, electrospinning and electrofusion techniques, which are either expensive or incompatible with mass production process, leading to high cost of the fabrication.[6-8] Moreover, the fabrication process of these devices may cause prodigious pollution to the environment. Thus, there is an urgent need to develop environmentally friendly supercapacitors using large-scale and low cost technologies.

To date, the development pursued in active material of supercapacitors mainly concerns high reversible capacitance, structural flexibility and stability, fast cation diffusion under high charge–discharge rates, and environmental friendliness. As a transition metal element, manganese can exist as a variety of stable oxides (MnO, Mn_3O_4, Mn_2O_3, MnO_2), which have significant predominance such as low cost, abundant resource, and high theoretical specific capacitance (1370 F/g).[9] In the last few years, several approaches, such as sol-gel route[10], anodic electrodeposition[11, 12], and cathodic electrodeposition[12] have been developed. Recently, the δ-MnO_2 nanosheets with an ultrathin thickness showing relatively large surface areas and porous structure turns out to be an ideal active material for supercapacitors. Recently, our group has developed an efficient, convenient and scalable technology for preparing the rGO/mixed-valent manganese oxides (rGO/MnO_x) composite with superior electrochemical properties, which is compatible to the slurry dispensing process for electrode fabrication.[13]

It is an interesting idea that paper, a commodity ubiquitous in everyday life, can be exploited for future electronics. The advantages are obvious: paper holds unique porous bulk structure and absorptive surface properties, which can introduce more electrochemically active surfaces for absorption/desorption of the electrolyte ions to facilitate charge transport during charging/discharging processes.[14] Moreover, the inexpensive and environmental-friendly nature of paper offers great opportunities for us to utilize it as the substrate of a supercapacitor.[15, 16] Our group has investigated, for the first time, the life cycle assessment of paper to quantify a paper-based printed-circuit-board's (PCB's) environmental impacts , and draw a conclusion that paper-based equipments are beneficial for a regional or global level of production.[17]

Here, we introduce an all-printed paper based supercapacitor (PPS) showing superior electrochemical performance assembled in an eco-friendly and easy-fabrication way. Using all-printed technologies, the PPS can be fabricated in mass production line, making it compatible with large-scale fabrication techniques, which has a great potential for industrialization.

II. EXPERIMENTAL

A. Synthesis of δ-MnO_2 nanosheets

Typically, 200 mL of DI water was added into a three-necked flask and heated to 90 °C with stirring. $KMnO_4$ (0.05 M, 100 mL) and $Mn(Ac)_2$ (0.05 M, 100 mL) solutions were added into the flask by a multi-channel peristaltic pump (Longerpump, BT100-1L) at a pumping speed of 0.5 mL min-1. Both chemicals reacted in the flask and formed MnO_2 nanosheets. After the reaction flask was cooled down to room temperature, the obtained solution was centrifuged (Bioridge, DD-5M) at a speed of 3600 rpm and washed three times by DI water. The as-prepared precipitation was freeze-dried (BMH Instruments, Alpha 1-2 LD plus) and was ready for use.

B. Preparation of the δ-MnO_2 cathode slurry

The δ-MnO_2 powder was mixed with 10 wt% of PVDF binder, 10 wt% of super P conductive agent and NMP

978-1-5386-2972-7/17/$31.00 ©2017 IEEE

solvent (3 mL) in a planetary rotator mixer (Hasai 300, China) for preparing the cathode slurry.

C. Preparation of the active carbon anode slurry

The activated carbon (AC) powder was mixed with 10 wt% of PVDF binder, 10 wt% of super P conductive agent and NMP solvent (3 mL) in a planetary rotator mixer (Hasai 300, China) for preparing the anode slurry.

D. Fabrication of PPS

Fabrication procedure of the paper-based PPS is shown in Figure 1.

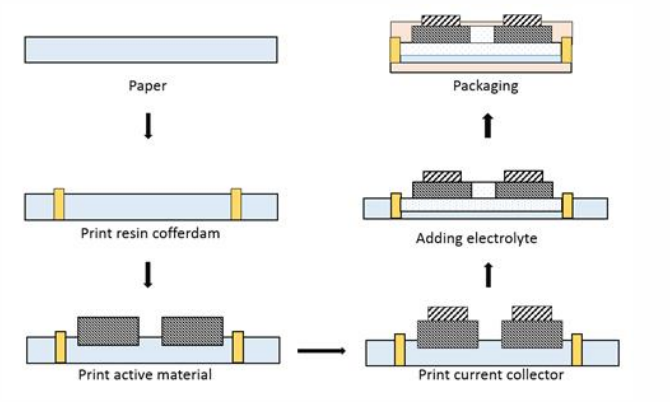

Fig.1 View of the fabrication procedure.

The paper was used as the substrate of the supercapacitor. Firstly, a commercial thermoplastic ink, set as the cofferdam, was screen printed and soaked by the paper, and the size of the outline border was 2.0*1.7 mm^2 with the width of ca. 0.2 mm. Then the cathode slurry and the anode slurry was stencil printed inside the cofferdam of the paper as the active material, the printing thickness was 0.2 mm before the slurry drying and shrinking. Each size for printing the slurry was 1.8*1.5 mm^2, the space between the two electrodes was controlled to be 1 mm to prevent short out happening caused by the flow of the slurry. Then the conductive carbon ink was screen printed onto the active material as the current collector. After drying, Na_2SO_4 aqueous electrolyte was added dropwise. Waiting for a moment till the electrolyte immersed into the active material, PDMS was coated over the device, leaving the current collector out of the surround of the glue.

E. Materials characterizations and electrochemical measurements.

The morphological characteristics of δ-MnO_2 were characterized by scanning electron microscopy (SEM, ZEISS SUPRA 55, 5 kV, Germany) and high-resolution transmission electron microscopy (HR-TEM, FEIG2 spirit, America). The surface species and chemical states of the sample were measured by X-ray photoelectron spectroscopy (XPS, ES-CALAB250Xi, Thermo Fisher Scientific, America). X-ray diffraction (XRD, RINT2000 V/PC, Bruker DS, Germany) was used to study the structures of the samples.

Electrochemical testings were performed on an electrochemical station (VMP3, Bio-Logic, France) with a three-electrode configuration. Cyclic voltammetry (CV), galvanostatic charging/discharging (GCD) and electrochemical impedance spectroscopy (EIS) of the as-prepared samples were investigated, respectively. The applied potential window of CV and GCD was in the range from 0 V to 0.8 V with Na_2SO_4 aqueous electrolyte. The EIS study was conducted in the frequency range between 100 KHz and 0.01 Hz with amplitude of 5 mV at an open-circuit potential. The mass capacitance (C_m), and the energy and power density (E and P) of supercapacitor were calculated by the equations as follows:

$$C_m = \frac{I \cdot \Delta t}{\Delta U \cdot m} \quad (1)$$

$$E = \frac{C_V \cdot (\Delta U)^2}{2 \cdot 3600} \quad (2)$$

$$P = \frac{E}{\Delta t} \quad (3)$$

where I is the applied current, Δt is the discharging time, ΔU is the operating voltage window, m is the total mass of mass materials.

III. RESULTS AND DISCUSSION

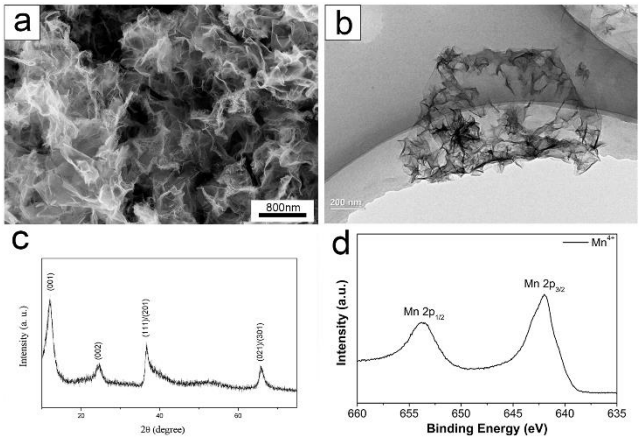

Fig.2 Morphological and structural characterizations of the materials. (a) SEM image of δ-MnO_2; (b) TEM image of δ-MnO_2; (c) XRD spectra of MnO_2; (d) XPS spectra of Mn 2p in MnO_2;

The morphology and microstructure of this MnO_2 were examined by SEM and TEM. As is shown in Fig 2a, the obtained MnO_2 showed a sheet-like structure, which enabled the ions easier to access the internal MnO_2 network and provided fast transport channels for ions. TEM image (inset of Fig. 2b) shows the manganese oxide nanosheets with the diameter in the range of 3-20 nm. Such structure with a high specific surface area is capable of providing fast ion transport channels; as a result, the electrolyte ions could easily access to the surface of the composite. XRD characterization revealed that MnO_2 (JCPDS NO.: 30-0820) is crystalline, as is shown in Fig 2c. Further valence state information of the

sample was obtained from XPS characterization, as shown in Fig.2d, the Mn 2p XPS spectrum exhibited two characteristic peaks at 638.7 eV, 642.6 eV, corresponding to spin-orbit peaks of manganese with valence states of +4.

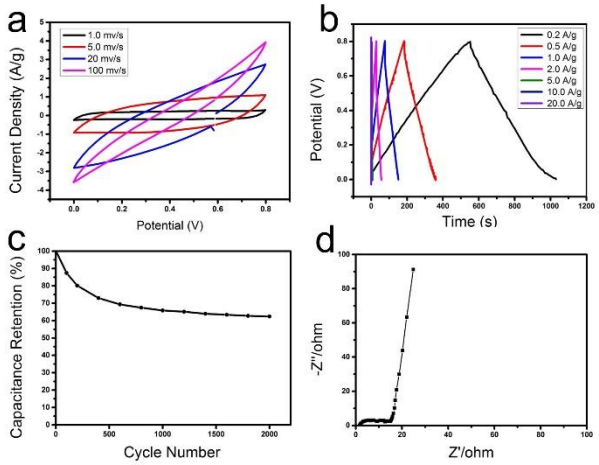

Fig.3 Electrochemical characterizations of the MnO_2 electrode in 0.5 M aqueous Na_2SO_4 electrolyte: (a) CV curves of the material at the scan rate between 1 to 100 mV s^{-1}; (b) GCD curves of the material at the scan rate between 0.2 to 20.0 A g^{-1}; (c) cycling performance of the electrode material; (d) Nyquist curve after the first cycle.

To evaluate the electrochemical performance of δ-MnO_2, CV, GCD and EIS testings were performed. The cyclic voltammetry (CV) of δ-MnO_2 was recorded in 0.5 M Na_2SO_4 aqueous solution, as shown in Figure 3a. The potential range was from 0.0 to 0.8 V vs Hg/HgO and different scanning rate were applied from 1 mV/s to 100 mV/s. It showed that the CV curves were relatively rectangular in shape and exhibited near mirror-image current response on voltage reversal, indicating a reversible reaction and ideal capacitive behavior of δ-MnO_2. With the increase of scanning rates, there is no significant change in rectangular shape, exhibiting high electrochemical reversibility in this potential range at high sweep rate. The GCD curves at different current densities are shown in Fig. 3b, which illustrated an almost-linear variation of potential during charging and discharging processes, further demonstrating the excellent capacitance behavior of this material. The charging and discharging time of δ-MnO_2 in this test was almost the same, indicating high reversibility and coulombic efficiency. The mass capacitance was up to 120 F/g at a current density of 0.2 A/g. What's more, the capacitance retention of δ-MnO_2 still remained 67.2% after 20,000 cycles at 100 mV/s scan rate, indicating relatively excellent cycling stability. In Fig. 3d, the frequency response analysis, in the frequency range between 10 mHz and 100 kHz with amplitude of 5 mV at an open-circuit potential, was conducted to study the alternating current impedance property of the MnO_2, the charge transfer resistance (R_{ct}) which caused by Faradic reactions on the surface was extremely low. The superior performance of the δ-MnO_2 is due to the following aspects: excellent electron and ion percolation network in the electrode material, the unique architecture and high specific surface area facilitating free access of electrolyte ions to the electrode surfaces, and the reduced diffusion length of the ions and electrons within the electrode phase.

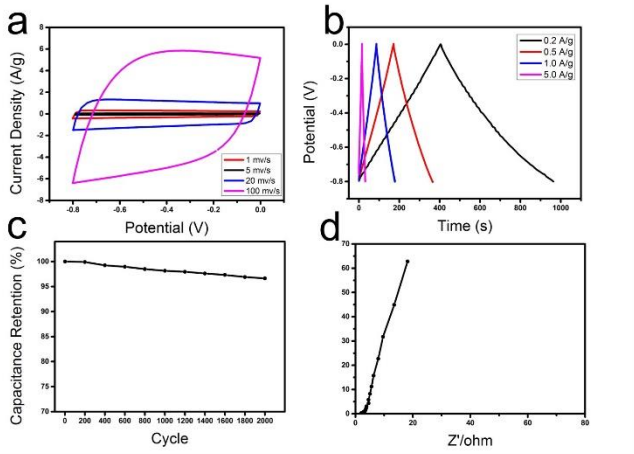

Fig.4 Electrochemical characterizations of the active carbon electrode in 0.5 M aqueous Na_2SO_4 electrolyte: (a) CV curves of the material at the scan rate between 1 to 100 mV s^{-1}; (b) GCD curves of the material at the scan rate between 0.2 to 5.0 A g^{-1} (c) cycling performance of the electrode material; (d) Nyquist curve after the first cycle.

For preparing an asymmetric paper based supercapacitor (PPS), AC slurry was used as anode material to couple with the corresponding MnO_2 slurry cathode. The electrochemical performance characteristic of the AC electrode is shown in Fig.4. This supercapacitor could double the size of working voltage window in an aqueous electrolyte, contributing to a dramatic improvement of both E_m and P_m values of the device. Fig. 5 illustrates the CV, GCD, EIS, and specific capacity of the device. This rate-dependent CV characterization of the PPS was performed under various scan rates ranging from 5 to 1000 mV s^{-1}, as shown in Fig. 4a. The GCD test was also performed to better characterize the electrochemical performance of the PPS device. As shown in Fig. 4c, the IR drop calculated from the GCD curve under 0.2 A/g was 0.2 V, suggesting a relatively low equivalent series resistance. Calculated from equation 1, C_m of the PPS reached a value of 4.7 mF g^{-1} based on the total active material of the device. The Nyquist plot of the sample was employed to evaluate the ionic mobility; inset of this figure is the magnified area in the high frequency range, from which the equivalent series resistance is very low, indicating that the PPS shows excellent ionic response at the high-frequency range. In the low frequency range, the Nyquist plot showed a nearly vertical line, indicating an ideal capacitive behaviour of the device. Specific capacitance C_m values versus scanning rate calculated by GCD study is shown in Fig.4d, conclusion can be drawn that with the increase of the scan rate, the C_m value decreased accordingly.

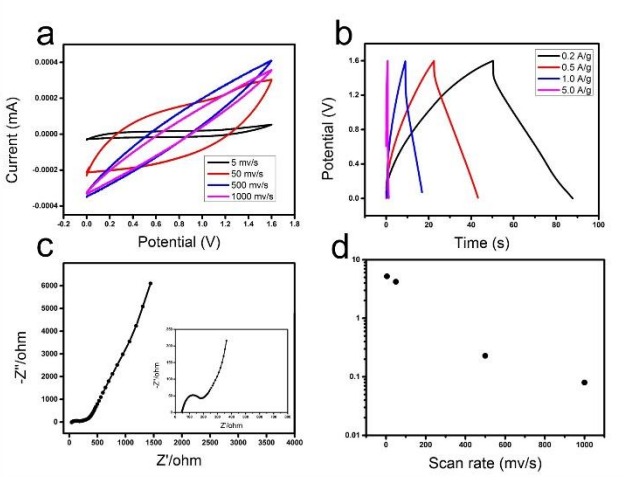

Fig.5 Electrochemical characterizations of the PPS in Na2SO4 electrolyte: (a) CV curves of the material at the scan rate between 5 to 1000 mV s-1; (b) GCD curves of the material at various scan rates; (c) Nyquist curve after the first cycle, inset is the expanded view of the high-frequency region; (d) Specific capacitance C_m values versus scanning rate calculated by GCD study;

IV. CONCLUSION

In summary, we introduce an all-printed paper based supercapacitor (PPS) assembled by screen printing and stencil printing technology, which provided the possibility of low cost and large-scale fabrication. The fabrication techniques proposed in this paper is through "top-down" microfabrication method, which can be further used in other micro-sized devices. The PPS with the volume of 2.0*1.7*0.2 mm^3 exhibit a very high mass capacitance up to 4.7 mF g^{-1} in Na_2SO_4 aqueous electrolyte. The high electrochemical performance of this device guarantees it a perfect candidate for applications in microelectronic systems or portable devices.

V.Acknowledgment

The authors thank the National Key Basic Research Program of China (Project No.2014CB932400), the National Nature Science Foundation of China (Project Nos. 51578310 & 51607102), China Postdoctoral Science Foundation (Project No. 2016M601001), Guangdong Province Science and Technology Department (Project Nos. 2015B010127009 & 2014B090917002 & 2015A030306010), Guangzhou Government (Project No. 201604016072), and Shenzhen Government (Project No. JCYJ20150518162144944) for financial supports.

VI. REFERENCES

[1] C. Wang, S. Wang, Y.-B. He, L. Tang, C. Han, C. Yang, *et al.*, "Combining Fast Li-Ion Battery Cycling with Large Volumetric Energy Density: Grain Boundary Induced High Electronic and Ionic Conductivity in Li4Ti5O12Spheres of Densely Packed Nanocrystallites," *Chemistry of Materials,* vol. 27, pp. 5647-5656, 2015.

[2] J. R. Miller and P. Simon, "Materials science. Electrochemical capacitors for energy management," *Science,* vol. 321, pp. 651-2, Aug 01 2008.

[3] P. Simon and Y. Gogotsi, "Materials for electrochemical capacitors," *Nature materials,* vol. 7, 2008.

[4] H. Tang, C. Yang, Z. Lin, Q. Yang, F. Kang, and C. P. Wong, "Electrospray-deposition of graphene electrodes: a simple technique to build high-performance supercapacitors," *Nanoscale,* vol. 7, pp. 9133-9, May 28 2015.

[5] B. Xie, C. Yang, Z. Zhang, P. Zou, Z. Lin, G. Shi, *et al.*, "Shape-Tailorable Graphene-Based Ultra-High-Rate Supercapacitor for Wearable Electronics," *ACS Nano,* vol. 9, pp. 5636-5645, 2015.

[6] K. U. Laszczyk, K. Kobashi, S. Sakurai, A. Sekiguchi, D. N. Futaba, T. Yamada, *et al.*, "Lithographically Integrated Microsupercapacitors for Compact, High Performance, and Designable Energy Circuits," *Advanced Energy Materials,* vol. 5, p. 1500741, 2015.

[7] C. Meng, J. Maeng, S. W. M. John, and P. P. Irazoqui, "Ultrasmall Integrated 3D Micro-Supercapacitors Solve Energy Storage for Miniature Devices," *Advanced Energy Materials,* vol. 4, p. 1301269, 2014.

[8] Y. Wang, X. Yang, A. G. Pandolfo, J. Ding, and D. Li, "High-Rate and High-Volumetric Capacitance of Compact Graphene-Polyaniline Hydrogel Electrodes," *Advanced Energy Materials,* vol. 6, p. 1600185, 2016.

[9] W. Wei, X. Cui, W. Chen, and D. G. Ivey, "Manganese oxide-based materials as electrochemical supercapacitor electrodes," *Chem Soc Rev,* vol. 40, pp. 1697-721, Mar 2011.

[10] C.-K. Lin, K.-H. Chuang, C.-Y. Lin, C.-Y. Tsay, and C.-Y. Chen, "Manganese oxide films prepared by sol–gel process for supercapacitor application," *Surface and Coatings Technology,* vol. 202, pp. 1272-1276, 2007.

[11] H. Gao, F. Xiao, C. B. Ching, and H. Duan, "High-performance asymmetric supercapacitor based on graphene hydrogel and nanostructured MnO2," *ACS Appl Mater Interfaces,* vol. 4, pp. 2801-10, May 2012.

[12] N. Nagarajan, M. Cheong, and I. Zhitomirsky, "Electrochemical capacitance of MnOx films," *Materials Chemistry and Physics,* vol. 103, pp. 47-53, 2007.

[13] Y. Wang, W. Lai, N. Wang, Z. Jiang, X. Wang, P. Zou, *et al.*, "A reduced graphene oxide/mixed-valence manganese oxide composite electrode for tailorable and surface mountable supercapacitors with high capacitance and super-long life," *Energy Environ. Sci.,* vol. 10, pp. 941-949, 2017.

[14] L. Yuan, X. Xiao, T. Ding, J. Zhong, X. Zhang, Y. Shen, *et al.*, "Paper-based supercapacitors for self-powered nanosystems," *Angew Chem Int Ed Engl,* vol. 51, pp. 4934-8, May 14 2012.

[15] B. Yao, L. Yuan, X. Xiao, J. Zhang, Y. Qi, J. Zhou, *et al.*, "Paper-based solid-state supercapacitors with pencil-drawing graphite/polyaniline networks hybrid electrodes," *Nano Energy,* vol. 2, pp. 1071-1078, 2013.

[16] Y. Z. Zhang, Y. Wang, T. Cheng, W. Y. Lai, H. Pang, and W. Huang, "Flexible supercapacitors based on paper substrates: a new paradigm for low-cost energy storage," *Chem Soc Rev,* vol. 44, pp. 5181-99, Aug 07 2015.

[17] J. Liu, C. Yang, H. Wu, Z. Lin, Z. Zhang, R. Wang, *et al.*, "Future paper based printed circuit boards for green electronics: fabrication and life cycle assessment," *Energy Environ. Sci.,* vol. 7, pp. 3674-3682, 2014.
[18] B. Ahmed, D. H. Anjum, Y. Gogotsi, and H. N. Alshareef, "Atomic layer deposition of SnO 2 on MXene for Li-ion battery anodes," *Nano Energy,* vol. 34, pp. 249-256, 2017.
[19] A. Balducci, R. Dugas, P. L. Taberna, P. Simon, D. Plée, M. Mastragostino, *et al.*, "High temperature carbon–carbon supercapacitor using ionic liquid as electrolyte," *Journal of Power Sources,* vol. 165, pp. 922-927, 2007.